Gettering of interstitial iron in silicon by plasma-enhanced chemical vapour deposited silicon nitride films

A. Y. Liu,[1] C. Sun,[1] V. P. Markevich,[2] A. R. Peaker,[2] J. D. Murphy,[3] and D. Macdonald[1]
[1]*Research School of Engineering, Australian National University, Canberra, Australian Capital Territory 2601, Australia*
[2]*Photon Science Institute, University of Manchester, Manchester M13 9PL, United Kingdom*
[3]*School of Engineering, University of Warwick, Coventry CV4 7AL, United Kingdom*

(Received 10 August 2016; accepted 3 November 2016; published online 18 November 2016)

It is known that the interstitial iron concentration in silicon is reduced after annealing silicon wafers coated with plasma-enhanced chemical vapour deposited (PECVD) silicon nitride films. The underlying mechanism for the significant iron reduction has remained unclear and is investigated in this work. Secondary ion mass spectrometry (SIMS) depth profiling of iron is performed on annealed iron-contaminated single-crystalline silicon wafers passivated with PECVD silicon nitride films. SIMS measurements reveal a high concentration of iron uniformly distributed in the annealed silicon nitride films. This accumulation of iron in the silicon nitride film matches the interstitial iron loss in the silicon bulk. This finding conclusively shows that the interstitial iron is gettered by the silicon nitride films during annealing over a wide temperature range from 250 °C to 900 °C, via a segregation gettering effect. Further experimental evidence is presented to support this finding. Deep-level transient spectroscopy analysis shows that no new electrically active defects are formed in the silicon bulk after annealing iron-containing silicon with silicon nitride films, confirming that the interstitial iron loss is not due to a change in the chemical structure of iron related defects in the silicon bulk. In addition, once the annealed silicon nitride films are removed, subsequent high temperature processes do not result in any reappearance of iron. Finally, the experimentally measured iron decay kinetics are shown to agree with a model of iron diffusion to the surface gettering sites, indicating a diffusion-limited iron gettering process for temperatures below 700 °C. The gettering process is found to become reaction-limited at higher temperatures. [http://dx.doi.org/10.1063/1.4967914]

I. INTRODUCTION

Iron is a harmful and common metallic impurity in the silicon materials used for solar cells and microelectronics.[1] In the solar cell fabrication process, the detrimental impact of iron is commonly mitigated by the gettering of iron to the heavily phosphorus doped regions near the wafer surfaces, during the high temperature phosphorus diffusion process used for the p-n junction formation.[1–5] Heavy boron diffusion or aluminium alloying processes could also achieve similar gettering effects, if well integrated into the solar cell fabrication processes.[1,3,4] In Czochralski silicon for microelectronics, the gettering of dissolved iron is commonly achieved by driving iron precipitation at intentionally introduced oxide precipitates in the silicon bulk, via low temperature annealing.[6–8] Similarly, in multicrystalline silicon materials for solar cells, the overall impact of iron can be alleviated by driving iron precipitation at the crystallographic defects,[9–12] although the process is much less effective than the high temperature phosphorus diffusion gettering approach.

Numerous studies have shown that annealing silicon wafers with plasma-enhanced chemical vapour deposited (PECVD) silicon nitride (SiN_x) films at high firing temperatures causes the concentration of dissolved iron (i.e., interstitial iron) in silicon to be reduced significantly.[13–17] The mechanism for this iron reduction has remained unresolved, and it has been hypothesised that it might be caused by the hydrogenation of iron in silicon.[13–17] This hypothesis was based on the reports that showed that the recombination activity and the concentration of interstitial iron in silicon were reduced after hydrogen incorporation, via exposure to hydrogen plasma,[18–20] hydrogen ion implantation,[21] wet chemical etching,[22] or deposition of PECVD silicon nitride films.[23] While there have been reports of the detection of new defect levels assigned to possible Fe-H complexes,[21–23] from theoretical calculations the binding energy of Fe-H pairs was found to be weak,[24] indicating the unlikelihood of the Fe-H pairs withstanding the relatively high temperatures used for firing. Others have suggested that the reduction was due to the accelerated precipitation of iron driven by hydrogen-enhanced iron diffusivity.[18] However, this hypothesis cannot explain the observed iron loss at higher annealing temperatures, at which the iron solubility limits were well above the dissolved iron concentrations in silicon, meaning that such an iron relaxation precipitation process should not proceed.

This work aims at uncovering the underlying mechanism responsible for the significant reduction of the interstitial iron concentration in silicon after annealing with PECVD SiN_x films. Secondary ion mass spectrometry (SIMS) analysis of the depth profile of iron was used to examine the distribution of iron in the annealed SiN_x film and the Si wafer substrate.

Deep-level transient spectroscopy (DLTS) was applied to the annealed silicon samples to determine whether any new defects with deep levels were formed. The SiN_x coated annealed samples were also subjected to further high temperature processes to monitor any changes in the interstitial iron concentrations. Finally, the experimentally measured iron decay kinetics at 250–900 °C were analysed using an iron diffusion model, and the fitted apparent diffusivities were compared to the reported iron diffusivities in the literature.

II. EXPERIMENT

A flowchart outlining the experimental procedures is shown in Fig. 1.

Boron-doped *p*-type float-zone (FZ) silicon wafers were used in this work. The samples in Experiments A, C, and D had a resistivity of 1.7 Ωcm and a thickness of 250 μm after chemical etching. The samples in Experiment B had a resistivity of 8 Ωcm and a thickness of 500 μm after etching.

Prior to iron implantation, the samples were chemically etched in an alkaline solution to remove saw damage, and were subsequently RCA cleaned. Iron implantation was carried out using relatively low implantation energy of 70 keV, with a beam current of around 50 nA scanned across a 3cm × 3cm aperture. The implanted doses of ^{56}Fe were 5×10^{11} cm^{-2} for the 500 μm thick wafers, and were varied from 5×10^{10} -2×10^{11} cm^{-2} for the 250 μm thick wafers. The samples were then annealed at 1000 °C for 3 h to uniformly distribute the implanted iron throughout the wafer thickness. The solubility limit of iron in silicon at 1000 °C is 4×10^{14}cm^{-3},[25] well above the target volumetric interstitial iron concentrations of 2×10^{12}–10^{13}cm^{-3}. Dry oxygen was used as the ambient gas for the anneal in order to facilitate the growth of silicon oxide layers of around 100 nm thick on the wafer surfaces, which not only acted as diffusion barriers for any possible furnace contamination, but also provided sufficient surface passivation for samples that were set aside as the silicon oxide (SiO_2) controls. The samples were cooled down from 1000 °C to 750 °C at a rate of 10 °C/min, before being removed from the furnace and cooled in high airflow to reach room temperature in minutes. A subset of the samples had the SiO_2 layers removed in dilute HF (1%) solution, and then received a shallow chemical etch in a HNO_3:HF (10:1) solution to remove any possible implantation damage near the surfaces, before being coated with PECVD silicon nitride films on both sides.

The silicon nitride films were deposited using an AK400 microwave/radio-frequency (μW/RF) PECVD reactor manufactured by Roth & Rau. The films were deposited at a substrate temperature of around 250 °C, under a pressure of 0.2 mbar, a μW plasma power of 500 W, and an RF bias voltage of 150 V. The NH3/SiH4/Ar gas flow was 20/20/20 sccm, respectively. The deposition time was 3 minutes. The resulting film thickness was 90 ± 20 nm, with a refractive index of 1.93 at a wavelength of 632 nm, a hydrogen content of ∼15%, and a Si-N bond density of $\sim 9 \times 10^{22}$ cm^{-3}. Note that the deposited SiN_x films were optimised for the surface passivation and anti-reflection purposes,[26,27] not for the most effective removal of iron from the silicon bulk.

A quasi-steady-state photoconductance (QSSPC) lifetime tester[28] from Sinton Instruments was used to measure the bulk minority carrier lifetime, and the interstitial iron concentration ($[Fe_i]$) was determined from the carrier lifetimes in the isolated Fe and FeB paired states.[29,30] Strong illumination was used to dissociate the FeB pairs.[31] The

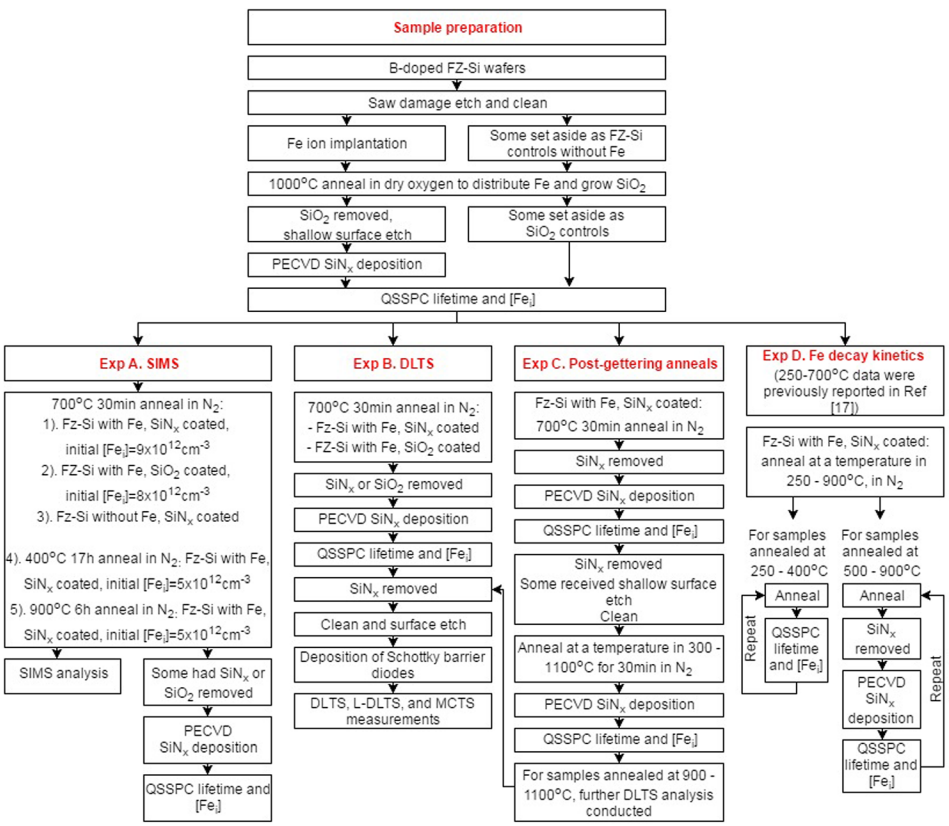

FIG. 1. Experimental procedure flowchart.

reported error bars in the measured interstitial Fe concentrations resulted from assuming a 10% uncertainty in the QSSPC lifetime measurements before and after dissociating FeB pairs.

The QSSPC lifetime technique is used throughout this work to measure the interstitial Fe concentration in silicon bulk. Interstitial Fe (Fe_i) refers to the total electrically active iron in silicon, which pairs with boron in the equilibrium state (i.e., in dark) forming Fe-B pairs.[25] In Experiment B, the DLTS technique is also used to determine the Fe_i concentration, from measuring the Fe-B concentration in samples kept in dark. SIMS measurements in Experiment A, however, detect the total concentration of Fe, regardless of the electrical state.

A. SIMS measurement of the re-distribution of iron

The following samples were prepared for SIMS analysis:

(1) Fe-implanted FZ-Si (initial $[Fe_i] = 9 \times 10^{12}\,cm^{-3}$), coated with PECVD SiN_x, annealed at 700 °C for 30 minutes in N_2;
(2) Fe-implanted FZ-Si (initial $[Fe_i] = 8 \times 10^{12}\,cm^{-3}$), coated with thermally grown SiO_2, annealed at 700 °C for 30 minutes in N_2;
(3) Clean FZ-Si with no Fe implantation, coated with PECVD SiN_x, annealed at 700 °C for 30 minutes in N_2;
(4) Fe-implanted FZ-Si (initial $[Fe_i] = 5 \times 10^{12}\,cm^{-3}$), coated with PECVD SiN_x, annealed at 400 °C for 17 hours in N_2;
(5) Fe-implanted FZ-Si (initial $[Fe_i] = 5 \times 10^{12}\,cm^{-3}$), coated with PECVD SiN_x, annealed at 900 °C for 6 hours in N_2.

The wafers were removed from the furnace at the respective annealing temperatures, followed by a rapid cool-down in high airflow within minutes. For the Fe-implanted samples annealed with the PECVD SiN_x films, the chosen annealing conditions were found to result in a significant reduction of the interstitial Fe concentration in silicon,[16,17] as will also be confirmed later in Sec. III. To monitor the changes in $[Fe_i]$, one set of the samples from each of the above processing conditions had the annealed SiN_x or SiO_2 layers removed and were re-passivated with PECVD SiN_x to enable QSSPC measurements of the bulk lifetime and $[Fe_i]$.

Another set of the samples with the annealed SiN_x or SiO_2 surface layers were sent to Evans Analytical Group (EAG) Laboratories for SIMS depth profiling of the iron concentration in SiN_x, or SiO_2, and the Si substrate. The nominal measurement depth resolution was better than 1.5 nm/step, although the actual resolution was limited by the mixing of bombarded ions during SIMS measurements. The detection limits for iron were about $3 \times 10^{14}\,cm^{-3}$ in SiN_x, $5 \times 10^{13}\,cm^{-3}$ in SiO_2, and $4 \times 10^{14}\,cm^{-3}$ in Si. Silicon was monitored as a marker species with its secondary ion intensity qualitatively measured, which served to distinguish the locations of SiN_x, or SiO_2, and the Si bulk in the depth profiles.

B. DLTS analysis

Iron implanted silicon wafers (initial $[Fe_i] = 10^{13}\,cm^{-3}$) with either PECVD SiN_x or thermally grown SiO_2 were annealed at 700 °C for 30 min in nitrogen. The annealed SiN_x or SiO_2 were then removed in dilute HF solution, followed by a re-passivation using PECVD SiN_x to allow QSSPC measurements of the bulk lifetime and $[Fe_i]$. After measurements, the SiN_x films were removed in dilute HF.

The samples were then chemically cleaned and etched again to remove about 45 μm from each surface in order to probe the bulk defect concentrations using DLTS. The wafers were subjected to a 1-min dip in dilute HF before the deposition of Schottky barrier diodes. The Schottky diodes of 1 mm diameter were formed on the *p*-type samples by plasma sputtering of Ti through a shadow mask. A layer of Au was evaporated onto the backside to form an Ohmic contact. Current-voltage (CV) and capacitance-voltage (*C-V*) measurements at different temperatures were carried out in order to check the quality of the diodes and to determine the concentration of non-compensated shallow acceptors/donors. Deep electronic levels were characterised with conventional deep level transient spectroscopy (DLTS), Laplace DLTS (L-DLTS),[32] and minority carrier transient spectroscopy (MCTS)[33] techniques. For the MCTS measurements, a flux of minority carriers for re-charging traps in the upper half of the Si bandgap was induced by backside light pulses from a 940 nm light-emitting diode.

C. Post-gettering anneals

Iron implanted silicon wafers (initial $[Fe_i]$ in the range of $(5–9) \times 10^{12}\,cm^{-3}$) with PECVD SiN_x were annealed at 700 °C for 30 min in nitrogen to reduce the interstitial iron concentrations. The annealed SiN_x films were stripped off in dilute HF, and the samples were re-passivated with SiN_x so that accurate QSSPC measurements of the silicon bulk were possible. The SiN_x films were stripped off again after QSSPC measurements, and the samples received a shallow chemical etch to remove any residual nitride films. Additional samples were included, which did not receive any surface etching after removing the SiN_x films in dilute HF.

The bare silicon wafers were chemically cleaned and were then subjected to annealing at a temperature in the range of 300–1100 °C for 30 min in nitrogen. Prior to the anneals, extended furnace cleaning was performed to minimise the impact of contamination for the bare silicon samples. Clean FZ-Si wafers with no iron implantation were co-processed in order to monitor the contamination levels in processing. The samples annealed at 300–900 °C were removed from the furnace at the respective annealing temperatures and were cooled down rapidly in a high airflow within minutes. The samples annealed at 1000 °C and 1100 °C were first cooled down to 900 °C in the furnace at a rate of about 15 °C/min, before being removed from the furnace at 900 °C and cooled down in high airflow. As the iron solubility at 900 °C (Ref. 25) is still above the interstitial iron concentrations in the samples, iron precipitation is not expected to occur during the cool-down to 900 °C. After annealing, PECVD SiN_x films were

deposited on all samples to allow QSSPC measurements of the bulk lifetime and [Fe_i].

DLTS analysis, as described above, was also carried out for the samples annealed at 900–1100 °C, in order to examine the defects in the silicon bulk.

D. Iron decay kinetics

The iron decay kinetics of the Fe-implanted FZ-Si samples annealed with PECVD SiN_x films at 250–700 °C were reported in Sun *et al.*,[17] and the data were imported in this work for re-analysis based on the new finding. In this work, we added in the decay kinetics data at 800 °C and 900 °C, using the same type of samples and the same experimental procedures as in Sun *et al.*[17] The process for preparing Fe-implanted FZ-Si wafers is as described above.

To measure the Fe reduction kinetics, as was conducted in Ref. 17 and in this work, the Fe-implanted silicon wafers (initial [Fe_i] in the range of 2×10^{12}–10^{13} cm^{-3}) with PECVD SiN_x films were annealed at temperatures in the range of 250–900 °C, and the interstitial iron concentrations with respect to the cumulative annealing time were measured using QSSPC. For samples annealed at temperatures of 500–900 °C, thermal-induced degradation of the SiN_x films was found to be severe and could affect the accuracy of the bulk lifetime measurements. These samples were therefore re-passivated with fresh SiN_x films after each annealing step. The samples annealed at 250–400 °C, on the other hand, did not need to be re-passivated after each incremental annealing time.

III. RESULTS

The initial interstitial iron concentrations in the FZ-Si wafers resulted from Fe ion implantation and the subsequent distribution anneal were found to be in the range of 2×10^{12}–10^{13} cm^{-3}, from QSSPC lifetime measurements. The measured interstitial Fe concentrations agree well with the implanted Fe dose.

A. SIMS measurement of the re-distribution of iron

Fig. 2 illustrates the changes in the interstitial iron concentration in the samples processed under the same conditions as those for SIMS analysis. The Fe_i concentrations were measured from QSSPC. These control samples had the same respective initial Fe_i concentrations as the samples for SIMS measurements, and therefore the observed different reductions in [Fe_i] in Fig. 2 indicate the different amounts of Fe_i loss from the Si bulk in the samples processed under different conditions. As shown in Fig. 2, significant reductions in the [Fe_i] can only be seen in the samples annealed with the SiN_x films, consistent with our previous reports.[16,17]

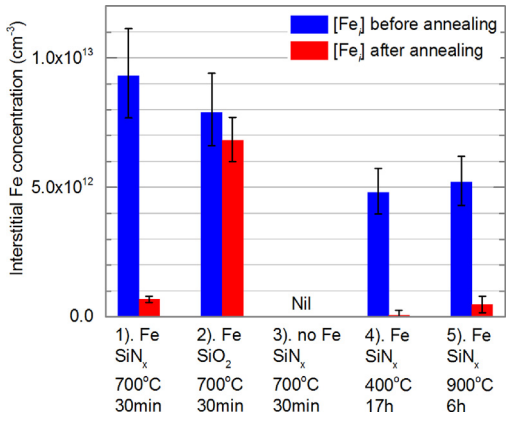

FIG. 2. QSSPC measured interstitial iron concentrations in the samples undergoing the same processes as those for SIMS analysis.

SIMS results are presented in Fig. 3, which illustrates the distribution of iron in the annealed SiN_x, or SiO_2, and the Si wafer bulk. Unlike QSSPC, SIMS is sensitive to the total Fe concentration, independent of its lattice location and clustering.

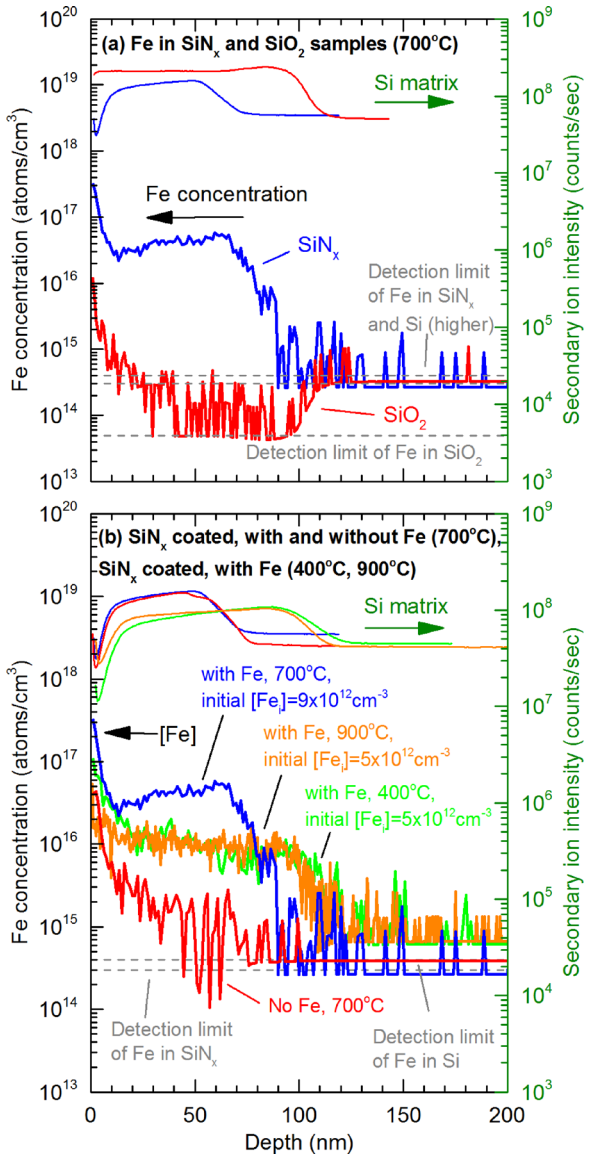

FIG. 3. SIMS depth profiles of the Fe concentration in (a) Fe-contaminated FZ-Si samples annealed with either SiN_x or SiO_2 surface layers at 700 °C for 30 minutes, with initial [Fe_i] of 9×10^{12} cm^{-3} and 8×10^{12} cm^{-3}, respectively; and (b) FZ-Si samples annealed with SiN_x at 700 °C for 30 minutes either with or without previous bulk Fe contamination; Fe-contaminated FZ-Si sample annealed with SiN_x at 400 °C for 17 hours, with an initial [Fe_i] of 5×10^{12} cm^{-3}; and Fe-contaminated FZ-Si sample annealed with SiN_x at 900 °C for 6 hours, with an initial [Fe_i] of 5×10^{12} cm^{-3}. The top curves in each subfigure are plotted against the vertical axis on the right, which indicate the positions of SiN_x, SiO_2, and Si in the depth profiles. The SIMS detection limits for the iron concentration in each material are denoted by the dashed lines.

As shown in Fig. 3(a), the Fe concentration in the SiN_x film is much higher than that in the SiO_2 layer. Note that the Fe concentrations are plotted on logarithmic scales. The Fe concentrations measured in the SiO_2 sample are at the detection limits in both the SiO_2 and the Si, apart from a narrow peak at the surface due to surface contamination occurring during transport and handling. Such a peak was observed in all samples examined in this work and is commonly observed in SIMS measurements. This low Fe concentration in the SiO_2 layer is consistent with the [Fe_i] measured from QSSPC as shown in Fig. 2, which revealed only a small drop in the bulk Fe_i concentration for the SiO_2 sample after the annealing process.

Fig. 3(b) shows both a comparison between two SiN_x-coated samples annealed for the same condition with and without previous bulk Fe contamination, and Fe-contaminated SiN_x-coated samples annealed at different temperatures. First, for the two samples annealed at 700 °C with and without previous bulk Fe contamination (blue and red curves), the Fe concentration in the SiN_x layer is found to be much higher in the sample with previous bulk Fe contamination than in the one without Fe in the Si bulk. This indicates that the higher Fe concentration in the SiN_x film does not arise from the PECVD SiN_x film growth process, but from Fe previously distributed in the Si bulk. In other words, the high Fe concentration in the SiN_x originates from the gettering of Fe from the Si bulk.

The amount of Fe in the annealed SiN_x film can be estimated from taking the difference of the area under the two Fe concentration curves in Fig. 3(b) (blue and red curves), giving a measure of Fe in atoms/cm^2. As the higher Fe concentration in the SiN_x comes from the Si bulk, re-distributing this Fe through the Si substrate of 250 μm, that is, dividing the Fe areal concentration by the wafer thickness, gives a volumetric Fe concentration of $9.5 \times 10^{12}\,cm^{-3}$. Given that the initial interstitial Fe concentration from QSSPC measurements was found to be $9.3 \times 10^{12}\,cm^{-3}$ (as shown in Fig. 2) and the same SiN_x films were deposited on both sides of the wafer, the amount of Fe gettered to the SiN_x on one side of the wafer is expected to be half of the estimated $9.5 \times 10^{12}\,cm^{-3}$ from the SIMS Fe profiles (Fig. 3(b)). However, considering the likely different composition of the SiN_x films used for SIMS quantitative calibration of the Fe concentration in SiN_x, which is based on electronic grade SiN_x instead of the solar grade SiN_x used in this work, this discrepancy in the Fe concentration is considered to be within an acceptable uncertainty range. In addition, it is possible that some of the bulk Fe was not in interstitial form and was hence not detectable previously by the QSSPC lifetime measurements, while SIMS detected the total Fe concentration. The quantitative SIMS iron profiles therefore further confirm that Fe in the Si bulk is gettered to the SiN_x film during annealing.

Second, Fig. 3(b) presents the SIMS Fe concentration profiles in Fe-contaminated SiN_x-coated samples annealed at a range of temperatures: 400 °C, 700 °C, and 900 °C. As was reported in our previous publications[16,17] and is also discussed later in Sec. III D, significant reductions of the bulk [Fe_i] have been observed in samples annealed with SiN_x at a wide range of temperatures from 250 °C to 900 °C. To examine whether or not the observed [Fe_i] reductions were caused by the same gettering effect, SIMS analysis was performed on the samples annealed at different temperatures. As shown in Fig. 3(b), the three samples annealed at different temperatures all demonstrate high Fe concentrations uniformly distributed in the annealed SiN_x films. Note that the two samples annealed at 400 °C and 900 °C had lower initial bulk Fe concentrations from lower Fe implantation dose, and the SiN_x films were thicker due to the variations in PECVD depositions. The detected Fe concentrations in the SiN_x films for the 400 °C and 900 °C samples are therefore lower than the 700 °C-annealed sample. The quantitative Fe concentrations in the annealed SiN_x films from SIMS measurements are $1.2 \times 10^{11}\,cm^{-2}$ and $1.0 \times 10^{11}\,cm^{-2}$ for the 400 °C and 900 °C, respectively, which correspond to $9.6 \times 10^{12}\,cm^{-3}$ and $8.0 \times 10^{12}\,cm^{-3}$ initial bulk Fe concentrations for the 250 μm thick wafers with SiN_x on both sides. SIMS estimation of the Fe concentrations is again larger than the QSSPC measurements by only a factor of 2, for the two samples annealed at 400 °C and 900 °C. Therefore, both the measured Fe profiles and the quantitative Fe concentrations from SIMS measurements on the samples annealed at different temperatures show the same gettering effect of the PECVD SiN_x films for Fe_i in Si, confirming that the observed [Fe_i] reductions in a wide temperature range (Refs. 16 and 17 and Sec. III D of this work) are caused by the same gettering mechanism.

As shown in Fig. 3(b), the concentrations of Fe appear to be fairly uniform in the annealed SiN_x films, with a slight tendency to increase towards the Si substrate for the 700 °C annealed sample. This uniform Fe distribution in the SiN_x indicates that the gettering process occurs via a segregation effect rather than via relaxation. Relaxation gettering relies on the existence of nucleation sites in silicon for the precipitation of supersaturated iron, in order to decrease the interstitial iron concentration towards the solubility limit. In clean FZ silicon, only the silicon surfaces, or in this case the interfaces between the silicon surfaces and the SiN_x films, could act as likely nucleation sites for iron precipitation. As the measured SIMS profile demonstrates a uniform Fe distribution in the SiN_x film rather than a concentration peak at the Si and SiN_x interface, the dominance of segregation gettering is apparent. Further evidence for the segregation gettering effect is shown in the comparison of the bulk Fe concentrations and the solubility limits, discussed later in Sec. III D.

B. Electrical activity from DLTS analysis

QSSPC lifetime measurements reveal that for the 500 μm thick wafers used for the DLTS analysis, annealing with PECVD SiN_x films at 700 °C for 30 min reduced the interstitial Fe concentrations from $10^{13}\,cm^{-3}$ to $(1–2) \times 10^{12}\,cm^{-3}$. On the other hand, the co-processed SiO_2 samples were found to maintain an unchanged Fe_i concentration of $10^{13}\,cm^{-3}$ after the 700 °C anneal.

The DLTS spectra (Fig. 4(a)) acquired from the bulk of the Fe-implanted FZ-Si samples annealed with either SiN_x or SiO_2 show that, first, except for the peak due to a donor level of the FeB defect, no other deep levels in the lower half of the bandgap were detected. Second, Fig. 4(a) demonstrates a much stronger magnitude of the FeB-related signal in the

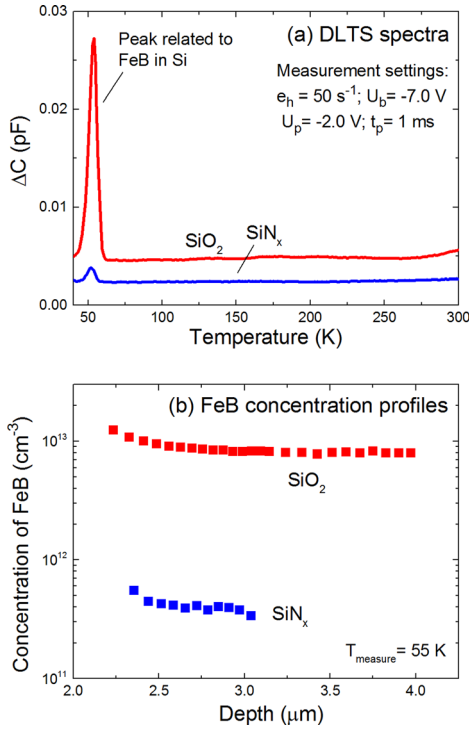

FIG. 4. (a) DLTS spectra measured on Fe contaminated silicon samples that were annealed with either SiN_x or SiO_2 surface layers at 700 °C for 30 mins. The spectra are shifted on the vertical axis for clarity. (b) The corresponding concentration profiles of the FeB pairs in these two samples. Prior to these measurements, 45 μm had been etched from each surface, and therefore, the depth in Figure 4(b) does not correspond to the depth scale in Fig. 3.

SiO_2 covered sample than in the SiN_x covered one. Note that in the DLTS measurements FeB was detected instead of interstitial Fe, as the samples were not deliberately illuminated to dissociate the FeB pairs. Under the measurement conditions used in this work, both methods give a measure of the electrically active iron in the silicon. Fig. 4(b) shows the concentration profiles of FeB in these two samples derived from L-DLTS and CV measurements at 55 K. The bulk concentrations of the FeB pairs, i.e., concentrations of interstitial iron in the pair dissociated state, are found to be 8×10^{12} cm^{-3} in the SiO_2 sample and 4×10^{11} cm^{-3} for the SiN_x sample, consistent in general with the interstitial iron concentrations determined from QSSPC lifetime measurements.

Further, we have tested the upper half of the bandgap with MCTS and observed only a peak due to the acceptor level of the FeB pairs with nearly the same magnitude ratio for the samples annealed with either SiO_2 or SiN_x surface layers as for the DLTS peak seen in Fig. 4(a) for the samples with the same dielectric layers.

C. Post-gettering anneals without SiN_x

The hypothesis of iron gettered by the PECVD silicon nitride films was ruled out in our previous publication[16] based on the experimental evidence reported by McLean *et al.*[15] In that work, it was reported that after removing the annealed SiN_x films, the reduced interstitial Fe concentrations recovered to the initial levels after a 900 °C anneal. This was interpreted as de-hydrogenation of the passivated iron. This experimental observation contradicts the finding in Sec. III A above, where we show that iron is gettered by the SiN_x films from SIMS measurements.

To clarify this discrepancy, McLean *et al.*'s experiment was replicated in this work. The Fe-implanted FZ-Si samples were first annealed with SiN_x to reduce the interstitial iron concentrations by two orders of magnitude, as shown in Fig. 5. The annealed SiN_x films were then removed, and the bare silicon samples were subjected to annealing at a temperature in the range of 300–1100 °C for 30 min in N_2. As shown in Fig. 5, the resulting interstitial Fe concentrations were found to remain largely unchanged compared to the post-gettered state. Samples with and without surface etching prior to the bare-Si anneals produced similar results. The slightly increased Fe_i concentrations after the 1000 °C and 1100 °C anneals (note that in Fig. 5 the Fe_i concentrations are plotted in logarithmic scale) are likely due to furnace contamination at the higher processing temperatures. This is supported by DLTS measurements of a co-annealed FZ-Si sample that was not Fe-implanted.

The lack of iron reappearance after the post-gettering anneals was also confirmed by DLTS analysis of the three samples annealed at 900–1100 °C. The DLTS peak due to the FeB pairs could not be detected in samples annealed at 900 and 1000 °C, and only a small FeB-related signal was observed in the sample annealed at 1100 °C. However, the same FeB defect signal was also detected in a clean FZ-Si control sample co-annealed at 1100 °C, indicating the probability of process contamination.

By carefully replicating McLean *et al.*'s experiment and extending it to a much wider annealing temperature range, we observe contrary experimental results. In McLean *et al.*'s work, the samples were not re-passivated after high temperature annealing, that is, the QSSPC measurements of the bulk carrier lifetime were made on the samples with much degraded surface passivation. The interstitial iron

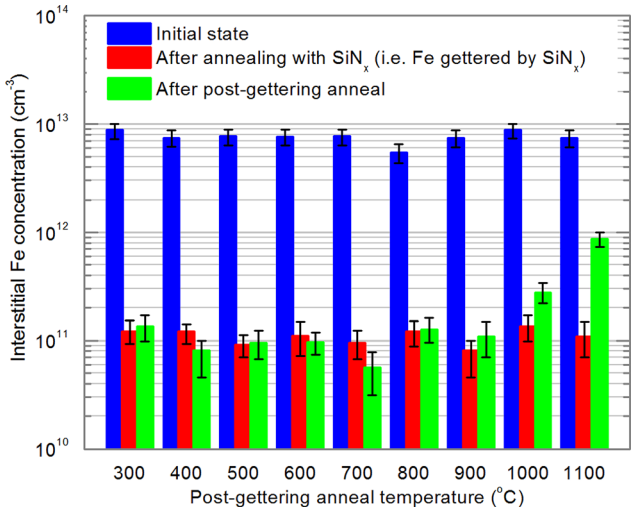

FIG. 5. Interstitial iron concentrations of Fe-implanted FZ-Si samples in the initial state, after annealing with SiN_x films at 700 °C for 30 minutes (which results in the gettering of iron by SiN_x), and after post-gettering annealing at 300–1100 °C with the previously annealed SiN_x films removed and the samples annealed as bare Si wafers.

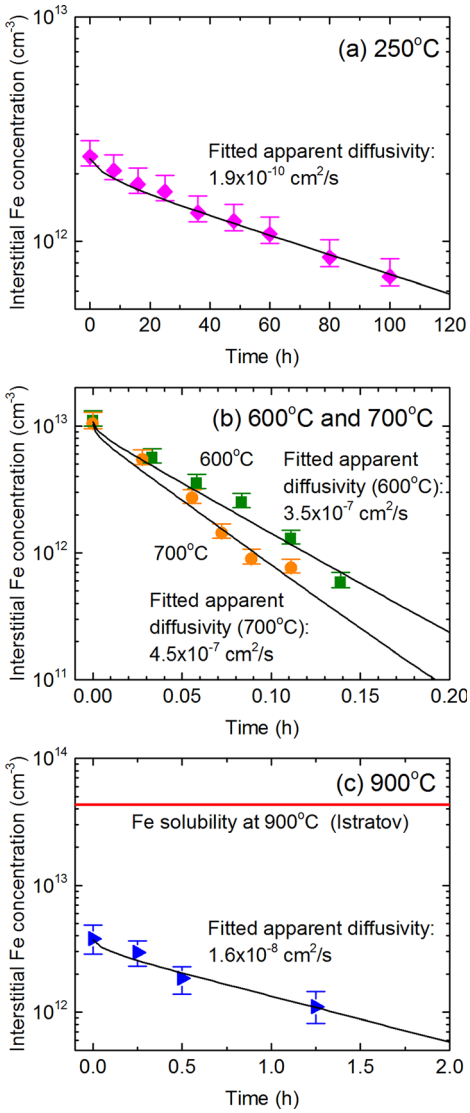

FIG. 6. Measured iron decay kinetics at (a) 250 °C,[17] (b) 600 °C and 700 °C,[17] and (c) 900 °C from annealing Si wafers coated with PECVD SiN_x films at the respective temperatures (symbols), and fits to the experimental data using a model of iron diffusion to the surface gettering sites (lines).[34] Iron solubility at 900 °C (Ref. 25) is included in Figure 6(c). Note that the magnitude scales on both axes differ in all three plots.

concentrations estimated from such measured lifetimes therefore suffer a large uncertainty and inaccuracy. The results of the carefully performed post-gettering anneals in this work further support the finding that Fe is gettered by the SiN_x films during annealing, and thus, no reappearance of iron is observed in any of the post-gettering annealed samples.

D. Interpretation of the measured iron decay kinetics

The decay kinetics of the interstitial iron concentration in silicon annealed with PECVD SiN_x films at 250–700 °C were presented in Ref. 17, and the data were incorporated in this work for re-analysis according to the new finding. This work extends the temperature range to 900 °C. A model of iron diffusion to the gettering sites on both wafer surfaces, described in Ref. 34, is used to fit the measured iron decay kinetics at 250–900 °C, with the apparent iron diffusivity being a fitting

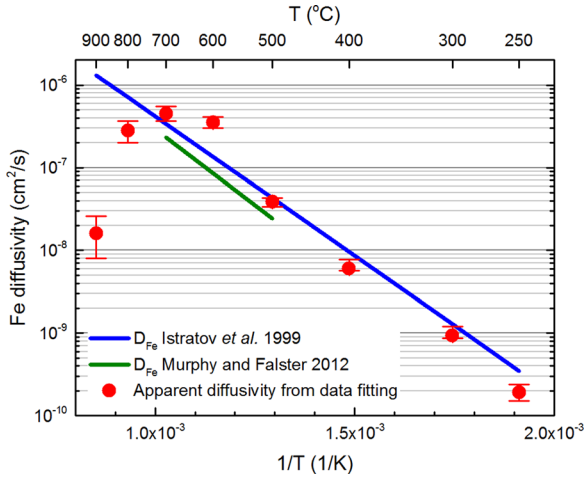

FIG. 7. Apparent diffusivities from fitting the experimental data of the iron decay kinetics with a model of iron diffusion to surface gettering sites (symbols),[34] and the reported iron diffusivities in the literature (lines),[25,34] at 250–900 °C. The kinetics data at 250–700 °C are imported from our previous work.[17]

parameter. The kinetics data can be well described by the model, as shown by some examples in Fig. 6.

Fig. 7 presents a comparison of the extracted apparent diffusivities at 250–900 °C with the literature values for the Fe diffusivities.[25,34] The fitted apparent diffusivities at 250–700 °C are shown to agree in general with the Fe diffusivities reported in the literature, indicating that the gettering process is likely diffusion-limited in this temperature range. Moreover, Sun *et al.*'s analysis of the iron decay kinetics at 250–700 °C gave an activation energy of 0.76 eV for the iron reduction process,[17] which is close to the iron diffusion activation energy of 0.67 ± 0.02 eV reported in Istratov *et al.*[25] and 0.73 ± 0.05 eV in Murphy and Falster.[34]

At higher temperatures of 800–900 °C, the gettering process becomes less effective, as revealed by the reduced fitted apparent diffusivities in Fig. 7, and also by comparing the iron decay kinetics at 600 °C, 700 °C (Fig. 6(b)), and 900 °C (Fig. 6(c)). The slower $[Fe_i]$ reduction processes are unlikely caused by the furnace contamination of iron at 800–900 °C, as the co-processed clean FZ-Si samples showed negligible rise in the Fe_i concentration. The reduced rate of the $[Fe_i]$ decay kinetics is possibly due to the gettering process becoming reaction-limited instead of diffusion-limited at higher temperatures as a result of the segregation ratio becoming less favourable for gettering, as also occurs for phosphorus diffusion gettering of iron,[1,2] for example.

In addition to the SIMS measurements of the Fe distribution in the annealed SiN_x films shown in Fig. 3, further evidence for segregation gettering is shown by comparing the Fe decay kinetics at 900 °C with the known Fe solubility[25] in Fig. 6(c). The solubility limit of Fe in silicon at 900 °C is $4 \times 10^{13} cm^{-3}$,[25] which is an order of magnitude higher than the initial interstitial Fe concentration of 4×10^{12} cm^{-3} in the sample. However, while being annealed with SiN_x films at 900 °C, some reduction of the interstitial Fe concentration takes place, as evident in Fig. 6(c). The capability to getter at high temperatures, where the solubility limit exceeds the dissolved

Fe concentration, is another indication that the gettering process is driven by the segregation effect, rather than relaxation.

IV. DISCUSSION

The results presented above clearly indicate that the significant reduction in the interstitial iron concentration in silicon wafers annealed with PECVD SiN_x films is caused by the segregation gettering of iron by SiN_x. This finding, however, does not contradict the reported possible Fe-H pairs in the literature,[21–24] which were shown to anneal out at temperatures above 175 °C,[22,23] agreeing with the theoretical calculations of the low binding energy of Fe-H pairs.[24]

Estreicher *et al.*[35] conjectured the formation of substitutional iron (Fe_s) in Si via the reaction of interstitial iron (Fe_i) with a pre-existing vacancy. According to Estreicher *et al.*'s predictions, Fe_s has an acceptor energy level in the upper half of the bandgap. Heat-treatments of Si samples covered with silicon nitride films deposited by low-pressure chemical vapour deposition (LPCVD) have been shown to result in supersaturation of vacancies in the silicon bulk.[36] Our SIMS measurements indicate that the formation of Fe_s is not a significant mechanism under the conditions of our experiments. Further, the DLTS/MCTS results strongly support our conclusion that the reduced interstitial iron concentration in the samples annealed with SiN_x films is not related to the formation of a new electrically active iron phase or complex in the silicon bulk.

The finding that interstitial iron is gettered by SiN_x films may help explain the discrepancy between the results of long, low temperature annealing experiments performed on multicrystalline silicon (mc-Si) by Krain *et al.*,[37] Liu and Macdonald,[9] and Al-Amin and Murphy.[12] Krain *et al.*[37] used SiN_x passivation and found a systematic reduction in interstitial iron, with the activation energy being close to the diffusion activation energy of iron. Liu and Macdonald[9] used thermally grown SiO_2 passivated mc-Si wafers and reported a systematic reduction in interstitial iron at a rate much slower than that reported by Krain *et al.*[37] Al-Amin and Murphy[12] applied temporary iodine-ethanol passivation at each processing step but did not find a systematic interstitial iron reduction. This current contribution shows that the role of external as well as internal gettering should be considered when SiN_x passivation is used. Guided by our current study, Al-Amin and Murphy recently applied SIMS depth profiling to a second set of mc-Si samples passivated with SiN_x films. Their new results broadly agree with our hypothesis, showing iron in the SiN_x film after low temperature annealing with the concentration dependent on annealing temperature.[38]

The underlying mechanism for the gettering effect of PECVD silicon nitride layers remains unclear at this stage. The gettering effect of Si_3N_4 layers, from chemical vapour deposition (CVD) at 700–800 °C, has been reported in the literature.[39–43] Annealing silicon with Si_3N_4 surface layers was shown to reduce the formation of stacking faults in the subsequent oxidation step,[39,40] as well as the microdefects in epitaxial layers on silicon.[41,42] Metallic impurities such as Cu and Au were found to be reduced.[39] While Petroff *et al.* conjectured the gettering mechanism to be due to the internal stress and non-stoichiometry of the Si_3N_4 films,[39] Jourdan *et al.* attributed the gettering effect to the Si_3N_4/Si interface which develops local stress and creates dislocations upon annealing.[43] In addition to the debated gettering mechanism of the CVD Si_3N_4 films, the PECVD SiN_x films deposited at low temperatures (below 300 °C in this study) have different properties to the CVD Si_3N_4 films deposited at 700–800 °C.[26,27] PECVD films are generally less dense and contain more defects and voids, which could aid their ability to segregate impurities. Further investigation is required to understand the details of the gettering mechanism of the PECVD silicon nitride and the effects of the film properties on the gettering efficiency.

Precipitation of iron at the Si/SiO_2 interface is a well-known effect.[1] This is not observed in the SIMS iron profile of the SiO_2 coated Si sample (Fig. 3(a)), most likely due to an insufficient degree of supersaturation of interstitial iron at 700 °C and an insufficient time of 30 minutes for the nucleation and growth of iron silicide.[1,9,25] The SIMS iron profiles also show that the SiO_2 layer is unlikely to have served as a segregation gettering layer for iron, as the iron concentration in SiO_2 remains below the detection limit. This agrees with the work by Smith *et al.*,[44] where the solubilities of iron in Si and SiO_2 were found to be similar. However, Ramappa and Henley[45] reported a strong tendency of iron to segregate into the SiO_2 layer. As discussed by Istratov *et al.* in a review paper of iron in silicon,[1] the interaction of iron with SiO_2 and Si is complex and may involve chemical binding reactions that are dependent on the specific process conditions.

Preliminary tests show that the atomic layer deposited (ALD) aluminium oxide films produce a similar iron decay rate at 400 °C (Ref. 9) compared to the PECVD SiN_x films,[16] suggesting that the ALD aluminium oxide may also act as a segregation gettering layer for iron. Similar SIMS profiling analysis could be used to confirm this hypothesis.

The benefits of firing multicrystalline silicon with PECVD silicon nitride films are generally attributed to the hydrogenation effect, and the gettering effect of the PECVD silicon nitride films has not been previously taken into consideration. In this work, we show that the SiN_x surface layers have the capability to getter dissolved iron in silicon, and the process is largely diffusion-limited at temperatures below 700 °C. This finding prompts us to speculate that the SiN_x films may be able to getter some very-fast-diffusing metallic impurities in silicon during firing, such as Cu and Ni, which could also contribute to the overall beneficial effect of firing defect-rich multicrystalline silicon wafers coated with PECVD silicon nitride films.

V. CONCLUSION

The disappearance of interstitial iron in silicon after annealing silicon wafers with PECVD silicon nitride films is found to be due to the segregation gettering of Fe by the SiN_x, as evidenced by SIMS depth profiling of the Fe concentration in the annealed SiN_x layer and the Si substrate. A high and uniformly distributed concentration of iron is measured in the annealed SiN_x films, and the iron concentrations from quantitative SIMS measurements match the losses of interstitial iron

from the silicon bulk measured by QSSPC. The finding that the interstitial Fe in the Si bulk can be effectively removed by the PECVD SiN_x films at elevated temperatures via a segregation gettering effect is further supported by the following experimental results: 1) DLTS analysis revealed no new defect levels in the silicon bandgap after annealing with SiN_x, 2) post-gettering anneals of the SiN_x-stripped silicon samples do not result in any reappearance of iron, and 3) the measured iron decay kinetics at 250–700 °C are consistent with a model of diffusion-limited gettering of iron to the wafer surfaces. The segregation gettering process is found to occur in a wide temperature range (250–900 °C), and the process becomes reaction-limited rather than diffusion-limited at higher temperatures (800–900 °C).

ACKNOWLEDGMENTS

This work has been supported by the Australian Renewable Energy Agency (ARENA) through project RND009. Author C. Sun acknowledges the financial support from Australian Centre for Advanced Photovolatics. The work in the UK was supported by the Engineering and Physical Sciences Research Council via the SuperSilicon PV project (EP/M024911/1). Access to the low-energy ion implantation system at the Department of Electronic Materials Engineering (ANU) is greatly appreciated. The authors would like to thank Dr. Yimao Wan (ANU) for sharing his knowledge on the PECVD silicon nitride deposition processes and film properties.

[1]A. A. Istratov, H. Hieslmair, and E. R. Weber, "Iron contamination in silicon technology," Appl. Phys. A **70**, 489–534 (2000).
[2]J. S. Kang and D. K. Schroder, "Gettering in silicon," J. Appl. Phys. **65**, 2974–2985 (1989).
[3]M. Seibt, A. Sattler, C. Rudolf, O. Voß, V. Kveder, and W. Schröter, "Gettering in silicon photovoltaics: Current state and future perspectives," Phys. Status Solidi A **203**, 696–713 (2006).
[4]S. P. Phang and D. Macdonald, "Direct comparison of boron, phosphorus, and aluminum gettering of iron in crystalline silicon," J. Appl. Phys. **109**, 073521 (2011).
[5]P. Manshanden and L. J. Geerligs, "Improved phosphorous gettering of multicrystalline silicon," Sol. Energy Mater. Sol. Cells **90**, 998–1012 (2006).
[6]D. Gilles, E. R. Weber, and S. Hahn, "Mechanism of internal gettering of interstitial impurities in Czochralski-grown silicon," Phys. Rev. Lett. **64**, 196–199 (1990).
[7]M. Aoki, A. Hara, and A. Ohsawa, "Fundamental properties of intrinsic gettering of iron in a silicon wafer," J. Appl. Phys. **72**, 895–898 (1992).
[8]H. Hieslmair, A. A. Istratov, S. A. McHugo, C. Flink, T. Heiser, and E. R. Weber, "Gettering of iron by oxygen precipitates," Appl. Phys. Lett. **72**, 1460–1462 (1998).
[9]A. Y. Liu and D. Macdonald, "Precipitation of iron in multicrystalline silicon during annealing," J Appl. Phys. **115**, 114901 (2014).
[10]W. Seifert, O. Vyvenko, T. Arguirov, M. Kittler, M. Salome, M. Seibt *et al.*, "Synchrotron-based investigation of iron precipitation in multicrystalline silicon," Superlattices Microstruct. **45**, 168–176 (2009).
[11]J. Bailey and E. R. Weber, "Precipitation of iron in polycrystalline silicon," Phys. Status Solidi A **137**, 515–523 (1993).
[12]M. Al-Amin and J. D. Murphy, "Increasing minority carrier lifetime in as-grown multicrystalline silicon by low temperature internal gettering," J. Appl. Phys. **119**, 235704 (2016).
[13]L. Geerligs, A. Azzizi, D. Macdonald, and P. Manshanden, "Hydrogen passivation of iron in multicrystalline silicon," in *13th Workshop on Crystalline Silicon Solar Cell Materials and Processes, Vail, Colorado* (2003), pp. 199–202.
[14]A. Azzizi, L. J. Geerligs, and D. Macdonald, "Hydrogen passivation of iron in crystalline silicon," paper presented at the 19th European Photovoltaic Solar Energy Conference, Paris (2004).
[15]K. McLean, C. Morrow, and D. Macdonald, "Activation energy for the hydrogenation of iron in P-type crystalline silicon wafers," Paper presented at the Conference Record of the 2006 IEEE 4th World Conference on Photovoltaic Energy Conversion.
[16]A. Liu, C. Sun, and D. Macdonald, "Hydrogen passivation of interstitial iron in boron-doped multicrystalline silicon during annealing," J. Appl. Phys. **116**, 194902 (2014).
[17]C. Sun, A. Liu, S. P. Phang, F. E. Rougieux, and D. Macdonald, "Charge states of the reactants in the hydrogen passivation of interstitial iron in P-type crystalline silicon," J. Appl. Phys. **118**, 085709 (2015).
[18]P. Karzel, A. Frey, S. Fritz, and G. Hahn, "Influence of hydrogen on interstitial iron concentration in multicrystalline silicon during annealing steps," J. Appl. Phys. **113**, 114903 (2013).
[19]A. J. Tavendale and S. J. Pearton, "Deep level, quenched-in defects in silicon doped with gold, silver, iron, copper or nickel," J. Phys. C: Solid State Phys. **16**, 1665 (1983).
[20]S. J. Pearton and A. J. Tavendale, "Electrical properties of deep silver- and iron-related centres in silicon," J. Phys. C: Solid State Phys. **17**, 6701 (1984).
[21]M. Kouketsu and S. Isomae, "Hydrogen passivation of iron-related hole traps in silicon," J. Appl. Phys. **80**, 1485–1487 (1996).
[22]T. Sadoh, K. Tsukamoto, A. Baba, D. Bai, A. Kenjo, T. Tsurushima *et al.*, "Deep level of iron-hydrogen complex in silicon," J. Appl. Phys. **82**, 3828–3831 (1997).
[23]S. Leonard, V. Markevich, A. Peaker, B. Hamilton, and J. Murphy, "Evidence for an iron-hydrogen complex in p-type silicon," Appl. Phys. Lett. **107**, 032103 (2015).
[24]M. Sanati, N. G. Szwacki, and S. Estreicher, "Interstitial Fe in Si and its interactions with hydrogen and shallow dopants," Phys. Rev. B **76**, 125204 (2007).
[25]A. A. Istratov, H. Hieslmair, and E. R. Weber, "Iron and its complexes in silicon," Appl. Phys. A **69**, 13–44 (1999).
[26]Y. Wan, K. R. McIntosh, and A. F. Thomson, "Characterisation and optimisation of PECVD SiNx as an antireflection coating and passivation layer for silicon solar cells," AIP Adv. **3**, 032113 (2013).
[27]Y. Wan, K. R. McIntosh, A. F. Thomson, and A. Cuevas, "Low surface recombination velocity by low-absorption silicon nitride on c-Si," IEEE J. Photovoltaics **3**, 554–559 (2013).
[28]R. A. Sinton and A. Cuevas, "Contactless determination of current–voltage characteristics and minority-carrier lifetimes in semiconductors from quasi-steady-state photoconductance data," Appl. Phys. Lett. **69**, 2510–2512 (1996).
[29]G. Zoth and W. Bergholz, "A fast, preparation-free method to detect iron in silicon," J. Appl. Phys. **67**, 6764–6771 (1990).
[30]D. H. Macdonald, L. J. Geerligs, and A. Azzizi, "Iron detection in crystalline silicon by carrier lifetime measurements for arbitrary injection and doping," J. Appl. Phys. **95**, 1021–1028 (2004).
[31]L. Geerligs and D. Macdonald, "Dynamics of light-induced FeB pair dissociation in crystalline silicon," Appl. Phys. Lett. **85**, 5227 (2004).
[32]L. Dobaczewski, A. R. Peaker, and K. Bonde Nielsen, "Laplace-transform deep-level spectroscopy: The technique and its applications to the study of point defects in semiconductors," J. Appl. Phys. **96**, 4689–4728 (2004).
[33]R. Brunwin, B. Hamilton, P. Jordan, and A. Peaker, "Detection of minority-carrier traps using transient spectroscopy," Electron. Lett. **15**, 349–350 (1979).
[34]J. D. Murphy and R. J. Falster, "The relaxation behaviour of supersaturated iron in single-crystal silicon at 500 to 750 [degree]C," J. Appl. Phys. **112**, 113506 (2012).
[35]S. Estreicher, M. Sanati, and N. G. Szwacki, "Iron in silicon: Interactions with radiation defects, carbon, and oxygen," Phys. Rev. B **77**, 125214 (2008).
[36]S. T. Ahn, H. W. Kennel, J. D. Plummer, and W. A. Tiller, "Film stress-related vacancy supersaturation in silicon under low-pressure chemical vapor deposited silicon nitride films," J. Appl. Phys. **64**, 4914–4919 (1988).
[37]R. Krain, S. Herlufsen, and J. Schmidt, "Internal gettering of iron in multicrystalline silicon at low temperature," Appl. Phys. Lett. **93**, 152108 (2008).
[38]M. Al-Amin and J. D. Murphy, "Passivation effects on low temperature gettering in multicrystalline silicon," IEEE J. Photovoltaics (to be published).

[39]P. M. Petroff, G. A. Rozgonyi, and T. T. Sheng, "Elimination of process-induced stacking faults by preoxidation gettering of si wafers: II. Process," J. Electrochem. Soc. **123**, 565–570 (1976).
[40]G. A. Rozgonyi and R. A. Kushner, "the elimination of stacking faults by preoxidation gettering of silicon wafers: III. Defect etch pit correlation with p-n junction leakage," J. Electrochem. Soc. **123**, 570–576 (1976).
[41]K. Tanno, F. Shimura, and T. Kawamura, "Microdefect elimination in reduced pressure epitaxy on silicon wafer by back damage-Si3 N 4 film technique," J. Electrochem. Soc. **128**, 395–399 (1981).
[42]M. C. Chen and V. J. Silvestri, "Post-epitaxial polysilicon and Si3 N 4 gettering in silicon," J. Electrochem. Soc. **129**, 1294–1299 (1982).
[43]C. Jourdan, J. Gastaldi, J. Derrien, M. Bienfait, and J. M. Layet, "Synchrotron x-ray topographic observation of defect evolution at the Si-Si3N4 interface," Appl. Phys. Lett. **41**, 259–261 (1982).
[44]A. R. Smith, R. J. McDonald, H. Manini, D. L. Hurley, E. B. Norman, M. C. Vella *et al*., "Low-background instrumental neutron activation analysis of silicon semiconductor materials," J. Electrochem. Soc. **143**, 339–346 (1996).
[45]D. A. Ramappa and W. B. Henley, "Diffusion of iron in silicon dioxide," J. Electrochem. Soc. **146**, 3773–3777 (1999).